Charge-induced ferromagnetic phase transition and anomalous Hall effect in full *d*-band nonmagnetic metals

Lei Wang (王蕾),[1] X. R. Wang,[2,3] Tai Min,[1,*] and Ke Xia[4,†]

[1]*Center for Spintronics and Quantum Systems, State Key Laboratory for Mechanical Behavior of Materials, Xi'an Jiaotong University, Xi'an, Shaanxi 710049, China*

[2]*Department of Physics, The Hong Kong University of Science and Technology, Clear Water Bay, Kowloon, Hong Kong, China*

[3]*HKUST Shenzhen Research Institute, Shenzhen 518057, China*

[4]*Shenzhen Institute for Quantum Science and Engineering, Department of Physics, Southern University of Science and Technology, Shenzhen 518055, China*

(Received 18 January 2019; revised manuscript received 31 May 2019; published 12 June 2019)

Motivated by the rich physics of electric-field control of magnetic properties observed in recent experiments, we use the first-principles calculations to investigate charge-transfer-induced magnetism of the full *d*-band nonmagnetic metals. A ferromagnetic phase transition initiated by an electric-field-induced charge transfer was found for all full *d*-band nonmagnetic metals. Beside the ordinary Hund's rules in Cu and Ag, a more complex correlation between the charge and the induced magnetization has been found, especially in Pd. The origin of the abnormal charge-induced magnetization is determined by the Coulomb interaction-induced instability of spin degeneracy at specific charges. In addition, a large nontrivial anomalous Hall effect has been discovered, and the sign of the anomalous Hall conductivity can change as charge number varies, a feature potentially useful for future spintronic applications.

DOI: 10.1103/PhysRevB.99.224416

I. INTRODUCTION

Phase transition is a long-last theme in condensed matter physics because of its importance in fundamental physics and applications. A phase transition can be classical when it is induced by the temperature, as well as quantum at zero temperature when it is triggered by other parameters such as chemical doping [1,2], geometry [3,4], light [5], pressure [6], and electric [7–9] and magnetic fields [10,11]. Quantum phase transitions is an active topic in the field of strongly correlated electron systems, but it is seldom studied in the field of traditional solid-state magnetism with many good reasons even though various tools, including electric field, are used to tune the magnetic material parameters. Recent quest of interactions between magnetic materials and heavy metals at their interfaces force us to re-examine many fundamental phenomena, including how the Hund's rules are modified by an electric field.

In spintronics, electric-field control of magnetic properties such as magnetic anisotropy [12–18] and synthetic antiferromagnetic heterostructures [19–21] has attracted much attention. Moreover, the electric field is capable of controlling the Curie temperature and the perpendicular magnetic anisotropy of normal ferromagnetic metals [22], Heusler alloys [23], surfaces [24], magnetic multiplayers [25], and even newly discovered two-dimensional ferromagnetic materials [26–28]. However, the applied electric field is generally used to control the magnetism of ferromagnetic materials with a partially filled *d* band.

Recently, two groups had reported electric-field-induced magnetism in nonmagnetic 5*d* transition metal Pt using ionic liquid gating technique [29–31] and extended to nonmagnetic 3*d* transition metal Cu [32]. Even though our previous naive calculations had already shown good agreement with the experiment in Pt [31] and Cu [32], the physical origin and universality of this phenomena still need to be investigated.

In this paper, we study the charge-controlled ferromagnetic phase transition in full *d*-band nonmagnetic metals (Cu, Ag, Au, Pd, and Pt) using the first-principles method. After analyzing the band structures and spin-density distributions, a clear physical picture of the charge-induced ferromagnetic phase transition has been obtained. In addition, we also found a nontrivial anomalous Hall effect in these charged magnetized metals by Berry curvature calculations. The calculated anomalous Hall conductivity can be up to three times larger than that in normal 3*d* magnetic transition metals, and its sign changes as the charges are removed. This charge-tuned anomalous Hall conductivity could be potentially useful in spin logics or spin memories.

II. MODEL AND METHOD

One possible way of varying electron numbers of atoms on a metallic thin film is thorugh electric gating. This can be realized by inserting an ionic liquid (IL) layer, e.g., $[DEME]^+[TFSI]^-$ or $[BMIM]^+[FeCl4]^-$ [29–32], between the bottom electrode and the metallic thin films (MTF) and applying a voltage V_g as shown in Fig. 1. As explained in Ref. [33], the charge states on the MTF surfaces depend

*tai.min@mail.xjtu.edu.cn
†xiak@sustc.edu.cn

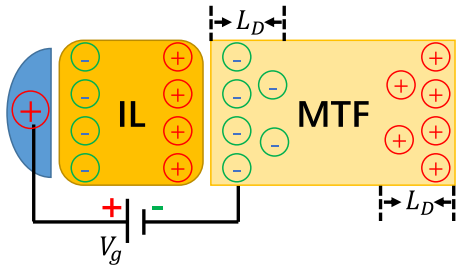

FIG. 1. Sketch of the model of the electric-field-induced charge accumulation in metallic thin films (MTF). As reported [29–32], an electric field is generated by an ionic liquid (IL) gating technique with an applied voltage V_g as shown in the figure. Under the electric field, the electrons in the MTF will be forced to move to bottom (left) surface, which left positive charge on the top (right) surface to balance the applied external electric field. The charge accumulation can only exist within the Debye length L_D on both surfaces.

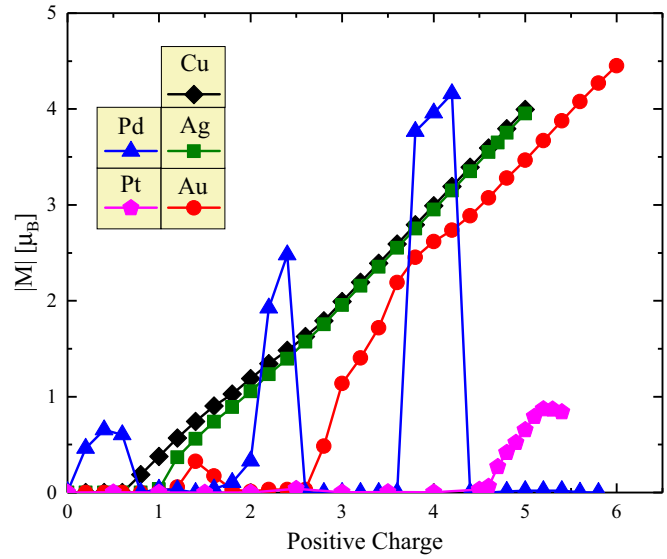

FIG. 2. The positive-charge-induced magnetic moment per atom for Cu, Ag, Au, Pd, and Pt. The positive charge means ionic states of the metals: a positive charge of 3 means removal of three electrons per atom, for example, Cu becomes Cu^{3+}.

on how a voltage is applied between two electrodes. In the following discussion, we will assume that the bottom electrode is grounded. Because of the electric screening effect in metals, electrons inside the MTF are accumulated on the bottom surface, and the holes are on the top surface under an external electric field from the IL gating voltage V_g such that a build-up internal electric field balances the applied external electric field. Obviously, it is difficult to create a large chemical potential difference or charge imbalance in the bulk of a metal, but a substantial amount of net charges (electrons or holes) can accumulate near the MTF surfaces within the Debye length L_D as shown in Fig. 1. Since the Debye length can vary from a few to tens of nanometers for different kinds of materials [34–36], the electron number on each atom in a nanometer-thick film can vary by a substantial value.

With the above consideration and under an applied IL gating voltage V_g, the charges will be accumulated inside the Debye length of the MTF bottom and top surface. If one treat the gating electrode and the thin film as an electric capactor with capactance C, the number of electrons (holes) on each atom in the thin film is $n = CV_g/N$, where N is the number of atoms in the films. Without losing generality, one can choose a proper unit for capacitance by setting $C/N = 1$, so that n and V_g is related to each other as $n = V_g$. Thus the atom X on the bottom surface becomes X^{n-} and the atom Y on the top surface becomes Y^{n+}, because of the loss of n electrons. It should be noted that the whole film is still charge neutral.

To carry out first principles calculations, it is convenient to set up a bulk model as the Debye length L_D can be much larger than the lattice constant discussed early. Because all the nonmagnetic metals studied in the work are face-centered cubic (fcc), it is enough and easier to use a simple unit cell in our calculations. Therefore, on top of all the above concepts, we can investigate the magnetic states of Cu, Ag, Au, Pd, and Pt inside the Debye length of both surfaces by adding or removing electrons on or from the atoms in one unit cell.

Obviously, Cu, Ag, Au, Pd, and Pt will not be magnetized by adding extra electrons because the d bands will be fully filled and the s electrons are too free to have localized magnetic moments. However, things are different when electrons are removed from the d bands, and the film can be nontrivially magnetized. For this reason, we mainly investigate the magnetization on the top MTF surface with positive charges in our study.

Technically, we carried out our first-principles calculations using the Vienna *ab-initio* simulation package (VASP) code [37,38], and all the calculations were based on DFT and the generalized gradient approximation with an interpolation formula according to Vosko, Wilk, and Nusair [39] and a plane-wave basis set within the framework of the projector augmented wave method [40,41]. The cut-off energy for the basis was 500 eV, and the convergence criterion for the electron density self-consistency cycles was 10^{-6} eV per atom. In the Brillouin zone, we sampled $(15 \times 15 \times 15)$ k-point grids using the Monk-horst-Pack scheme [42] to make sure the results converged. Also for convenient of the further study of the anomalous Hall effect, the spin-orbit coupling was also considered.

III. FERROMAGNETIC PHASE TRANSITION

As shown in Fig. 2, the magnetic moment per atom for Cu (black diamonds), Ag (green cubics), Au (red cycles), Pd (blue triangles), and Pt (magenta pentagons) were plotted as a function of positive charge. It shows that a normal metal become a ferromagnetic material as electrons are removed from the system, and the magnetic moments per atom are comparible and can be even larger than that of traditional magnetic elements. Normally, Cu and Ag follow the Hund's rules as shown in Fig. 2, in which their magnetic moment increases monotonically with the increase of the positive charges below the half-filling of the $3d$ and $4d$ bands. However, the charge-dependent magnetic moment does not obey the Hund's rules in other metals, especially for Pd. Three unexpected peaks appear, and a strangely sharp transition around Pd^{4+},

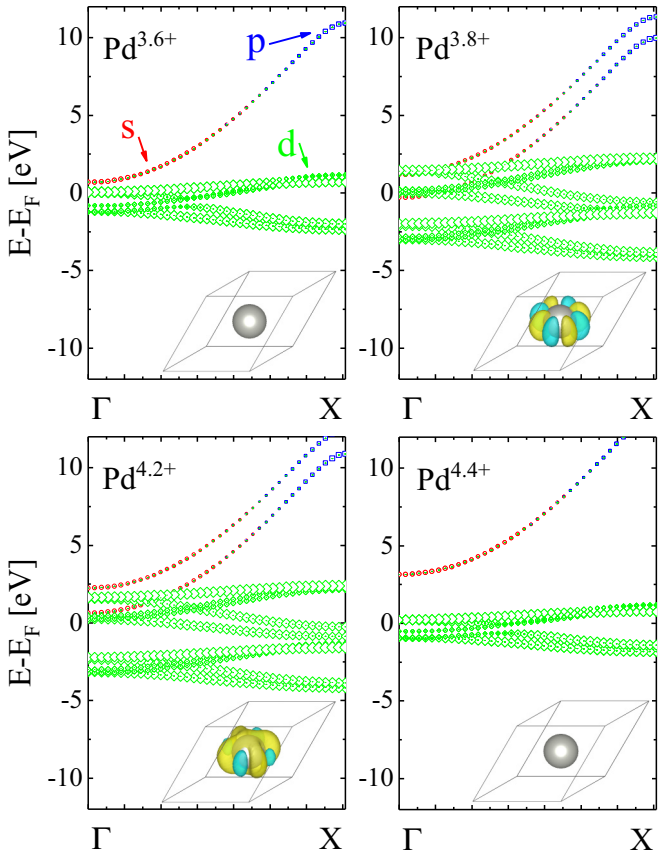

FIG. 3. The band structures of Pd^{n+} around Pd^{4+} for s (red cycles), p (blue cubics), and d- (green diamonds) orbits. The insets are the corresponding spin-density distribution in a single unit cell. The yellow and cyan denote spin-up and spin-down with isosurfaces of $0.0005a_0^{-3}$, where a_0 is the Bohr radius.

indicating a new control parameter for the ferromagnetic phase transition.

To understand the underneath physical origin of the magnetic moment jumps of Pd near electron removal of 3.8 and 4.2, we calculated the band structures of Pd^{n+} around Pd^{4+} and plotted them in Fig. 3. Also the corresponding spin-density distributions are shown in the insets. Clearly, one can see that, for $Pd^{3.6+}$ that does not have net magnetic moment as shown in Fig. 2, all five d bands are spin degenerated. However, for $Pd^{3.8+}$, the spin degeneracy of d bands are broken and 10 spin-resolved d bands are shown in Fig. 3 due to the Coulomb interaction induced the instability of spin degeneracy. Correspondingly, a nontrivial spin-density distribution in real space is clearly seen in the inset of Fig. 3. Similarly, for $Pd^{4.2+}$, there still exist 10 spin-resolved d bands; however, the spin-splitting energy of $Pd^{4.2+}$ is a little bit larger than that of $Pd^{3.8+}$, and so as the difference between the density of spin-up (yellow) and spin-down (cyan) as shown in Fig. 3 and its insets, which end up with a slightly rising of the magnetic moment. After $Pd^{4.4+}$, the magnetic moment fall back to zero because that the spin-up and spin-down are degenerated again. In this sense, the charge-related Coulomb interaction should be the origin of instability of spin degeneracy in charged Pd, which causes the unusual behavior in the charge-dependent magnetization of Pd in Fig. 2, as in Au and Pt, which are all beyond Hund's rules. However, more analytical works should be done to find a deeper explanation and obtain a critical relation between the charge and spin degeneracy.

Another important issue is whether the magnetic property lay on the ground state, otherwise the magnetic state will not be stable. Therefore, we recalculate the total energy E_0 with nonmagnetic assumption, and together with the original total energy E_m with magnetic assumption, the energy difference $\Delta E = E_m - E_0$ can be obtained as shown in Fig. 4, from which one can find that the tendency for Cu, Ag, Pd, Pt, and Au in Fig. 4 show good agreement with that in the charge-dependent magnetization in Fig. 2 for all positive charge, and with the negative value of ΔE, the magnetic ground states have been verified for all magnetic case in Fig. 2.

IV. ANOMALOUS HALL EFFECT

The anomalous Hall effect [43–46] is a very efficient way to verify the previous ferromagnetic phase transition by measuring the anomalous Hall conductivity σ^{AH}. An efficient way to calculate the anomalous Hall conductivity is of the Berry curvature formula [47,48] that in the case of magnetization parallel to z direction, reads

$$\sigma^{\mathrm{AH}} = -\frac{e^2}{\hbar}\int_{\mathrm{BZ}}\frac{d^3k}{(2\pi)^3}\Omega^z(\mathbf{k}), \tag{1}$$

where $\hbar$ is the Planck constant, "BZ" represent the integration over the total Brillouin zone, k is the wave vector, and $\Omega^z(\mathbf{k})$ is the sum of the Berry curvatures over the occupied bands for each $\mathbf{k}$:

$$\Omega^z(\mathbf{k}) = \sum_n f_n\Omega_n^z(\mathbf{k}), \tag{2}$$

with the band number n and the corresponding equilibrium Fermi-Dirac distribution function f_n, and the Berry curvature arises from the Kubo-formula derivation [49]:

$$\Omega_n^z(\mathbf{k}) = -\sum_{n'\neq n}\frac{2\mathrm{Im}\langle\psi_{n\mathbf{k}}|v_x|\psi_{n'\mathbf{k}}\rangle\langle\psi_{n'\mathbf{k}}|v_y|\psi_{n\mathbf{k}}\rangle}{(\omega_{n'}-\omega_n)^2}, \tag{3}$$

where the energy of each band $E_n = \hbar\omega_n$, $v_{x,y}$ are velocity operators and ψ is the wave function.

The above formula had already been generated in an open-source code WANNIER90 [50] with the maximally localized generalized Wannier functions (MLWFs) [51–53] which can connect to our previous VASP results. In addition, the direction of the magnetization is parallel to the fcc (001) direction, which is the z axis in our global coordinate system, and we used a $200\times200\times200$ k-point mesh in the total Brillouin zone together with adding a $5\times5\times5$ fine mesh around those points where $|\Omega^z(\mathbf{k})|$ exceeds 100 bohr^2 to make sure the Berry curvature calculations converged. The calculated anomalous Hall conductivity $\sigma_{xy}^{\mathrm{AH}}$ had been plotted in Fig. 5 for some typical points of Cu, Ag, Au, Pd, and Pt with nonzero magnetization, respectively.

From Fig. 5, the anomalous Hall conductivity show much more complex behavior than the magnetization in Fig. 2, which could even change the sign when changing the positive charge of the ions. However, notice that the sign changing in

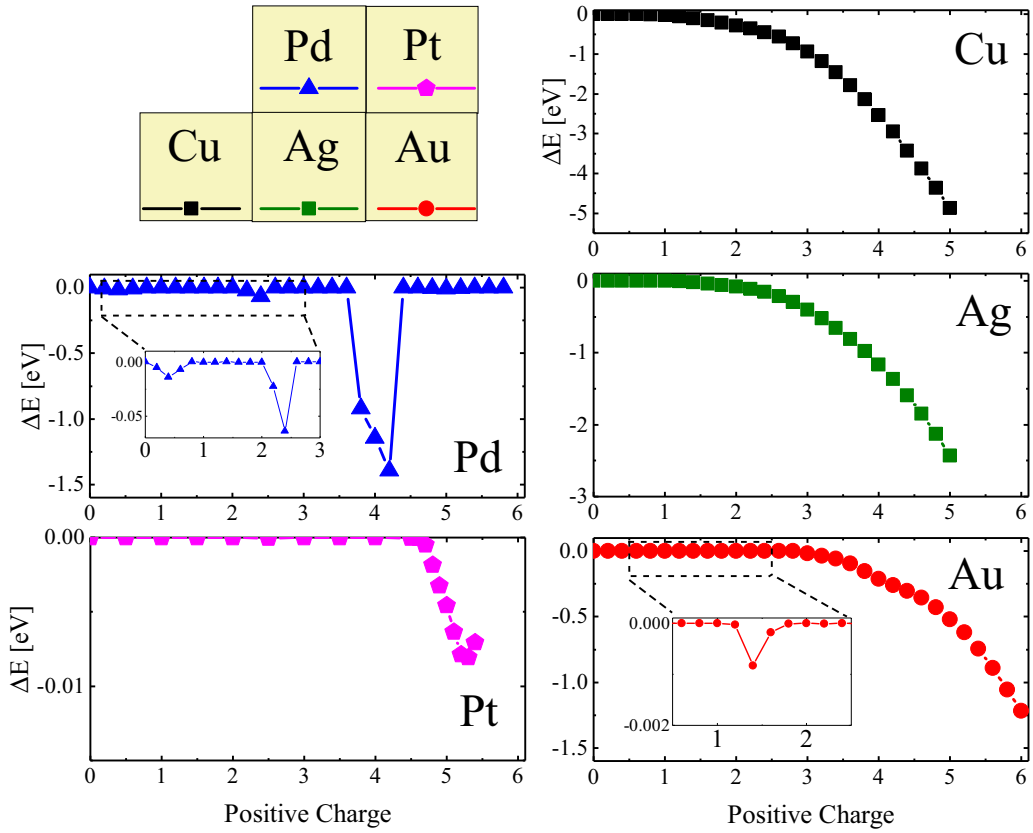

FIG. 4. The energy difference per atom $\Delta E = E_m - E_0$ of Cu, Ag, Au, Pd, and Pt as a function of the positive charge, where E_m and E_0 are, respectively, the total energy with and without spin polarization.

spin Hall effect had already been reported by first-principles calculation [54,55] with changing the referred Fermi energy.

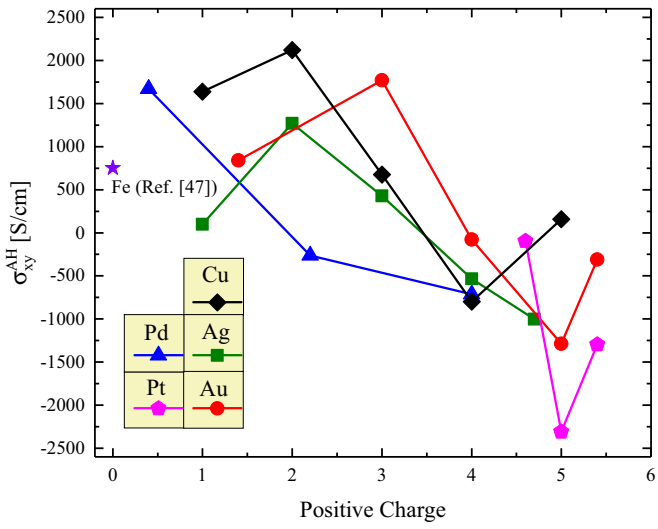

FIG. 5. The anomalous Hall conductivity (σ_{xy}^{AH}) of Cu, Ag, Au, Pd, and Pt as a function of the positive charge, where the spin polarization is along fcc (001) direction (the z axis). To show nontrivial anomalous Hall effect, few typical points from Fig. 2 with nonzero magnetic moment are used to calculate the anomalous Hall conductivity. A reported σ_{xy}^{AH} of Fe [47] was also included for a comparison.

Thus, because the origin of the anomalous Hall effect is quite similar with the spin Hall effect, and the "positive charge" is also another kind of moving the Fermi energy in the band structure, then the sign change of σ_{xy}^{AH} in our calculation in Fig. 5 can be understood in a similar way. Moreover, we notice that for Cu, Ag, Au, Pd, and Pt, the anomalous Hall conductivity can be even larger than three times of that in Fe, which is 751 S/cm from the Berry curvature calculation at zero temperature [47]. These larger anomalous Hall conductivity could be much more useful in spintronics devices, and if one can generate an adjustable external electric field on such thin film to induce positive charge as our calculation, then the sign change of the anomalous Hall conductivity could be use to make new types of spin logic or spin memory.

V. CONCLUSION

In conclusion, we found the charge-induced magnetism in full d-band nonmagnetic Cu, Ag, Au, Pd, and Pt metals from first-principles calculations. The metals, especially Pd, show complicated characteristic behavior beyond the conventional Hund's rules. The complicated behavior can be understood from the Coulomb interaction-induced instability of spin degeneracy. The nontrivial anomalous Hall effect can be three times larger than the normal 3d ferromagnetic material Fe. Our works reveal the physical origin of the charge-induced ferromagnetic phase transition of full d-band nonmagnetic metals, which has potential applications in future spintronics devices.

ACKNOWLEDGMENTS

This work was supported by the National Natural Science Foundation of China (Grant No. 11804266), the National Key Research and Development Program of China (Grants No. 2018YFB0407600 and No. 2016YFA0300702), and Shaanxi Province Science and Technology Innovation Project (Grant No. 2015ZS-02). K.X. is supported by the National Natural Science Foundation of China (Grants No. 61774017 and No. 11734004). X.R.W. is supported by Hong Kong RGC (Grants No. 16301518 and No. 16300117).

[1] C. P. Adams, J. W. Lynn, V. N. Smolyaninova, A. Biswas, R. L. Greene, W. Ratcliff, S.-W. Cheong, Y. M. Mukovskii, and D. A. Shulyatev, Phys. Rev. B **70**, 134414 (2004).
[2] D. Kim, B. Revaz, B. L. Zink, F. Hellman, J. J. Rhyne, and J. F. Mitchell, Phys. Rev. Lett. **89**, 227202 (2002).
[3] L. Vitos, B. Johansson, and J. Kollár, Phys. Rev. B **62**, R11957 (2000).
[4] S. M. Zhou, Y. Q. Guo, J. Y. Zhao, C. L. Wang, L. F. He, and L. Shi, J. Appl. Phys. **111**, 056104 (2012).
[5] M. Baran, S. L. Gnatchenko, O. Y. Gorbenko, A. R. Kaul, R. Szymczak, and H. Szymczak, Phys. Rev. B **60**, 9244 (1999).
[6] P. Sarkar, S. Arumugam, P. Mandal, A. Murugeswari, R. Thiyagarajan, S. Esaki Muthu, D. Mohan Radheep, C. Ganguli, K. Matsubayshi, and Y. Uwatoko, Phys. Rev. Lett. **103**, 057205 (2009).
[7] T. Lottermoser, T. Lonkai, U. Amann, D. Hohlwein, J. Ihringer, and M. Fiebig, Nature (London) **430**, 541 (2004).
[8] A. Zhou, W. Sheng, and S. J. Xu, Appl. Phys. Lett. **103**, 133103 (2013).
[9] M. Otani, Y. Takagi, M. Koshino, and S. Okada, Appl. Phys. Lett. **96**, 242504 (2010).
[10] S. Giri, P. Dasgupta, A. Poddar, A. Nigam, and T. Nath, J. Alloys Compd. **582**, 609 (2014).
[11] C. Koch, Mater. Sci. Eng.: A **287**, 213 (2000).
[12] P. Khalili and K. Wang, in *Proceedings of the 2015 4th Berkeley Symposium on Energy Efficient Electronic Systems (E3S)* (IEEE, New York, 2015).
[13] P. Khalili and K. L. Wang, in *Proceedings of the 2015 IEEE International Magnetics Conference (INTERMAG'15)* (IEEE, New York, 2015).
[14] B. Peng, Z. Zhou, T. Nan, G. Dong, M. Feng, Q. Yang, X. Wang, S. Zhao, D. Xian, Z.-D. Jiang, W. Ren, Z.-G. Ye, N. X. Sun, and M. Liu, ACS Nano **11**, 4337 (2017).
[15] U. Bauer, M. Przybylski, and G. S. D. Beach, Phys. Rev. B **89**, 174402 (2014).
[16] K. Kita, D. W. Abraham, M. J. Gajek, and D. C. Worledge, J. Appl. Phys. **112**, 033919 (2012).
[17] K. Ohta, T. Maruyama, T. Nozaki, M. Shiraishi, T. Shinjo, Y. Suzuki, S.-S. Ha, C.-Y. You, and W. Van Roy, Appl. Phys. Lett. **94**, 032501 (2009).
[18] Q. Yang, T. Nan, Y. Zhang, Z. Zhou, B. Peng, W. Ren, Z.-G. Ye, N. X. Sun, and M. Liu, Phys. Rev. Appl. **8**, 044006 (2017).
[19] X. Wang, Q. Yang, L. Wang, Z. Zhou, T. Min, M. Liu, and N. X. Sun, Adv. Mater. **30**, 1803612 (2018).
[20] Q. Yang, L. Wang, Z. Zhou, L. Wang, Y. Zhang, S. Zhao, G. Dong, Y. Cheng, T. Min, Z. Hu, W. Chen, K. Xia, and M. Liu, Nat. Commun. **9**, 991 (2018).
[21] R. Hao, L. Wang, and T. Min, IEEE Trans. Magn. **55**, 3400506 (2019).
[22] D. Chiba, S. Fukami, K. Shimamura, N. Ishiwata, K. Kobayashi, and T. Ono, Nat. Mater. **10**, 853 (2011).
[23] H. L. Wang, Y. Wu, H. J. Yu, Y. Jiang, and J. H. Zhao, J. Appl. Phys. **120**, 093901 (2016).
[24] S. Zhao, Z. Zhou, B. Peng, M. Zhu, M. Feng, Q. Yang, Y. Yan, W. Ren, Z.-G. Ye, Y. Liu, and M. Liu, Adv. Mater. **29**, 1606478 (2017).
[25] S. Zhao, L. Wang, Z. Zhou, C. Li, G. Dong, L. Zhang, B. Peng, T. Min, Z. Hu, J. Ma, W. Ren, Z.-G. Ye, W. Chen, P. Yu, C.-W. Nan, and M. Liu, Adv. Mater. **30**, 1801639 (2018).
[26] Y. Deng, Y. Yu, Y. Song, J. Zhang, N. Z. Wang, Z. Sun, Y. Yi, Y. Z. Wu, S. Wu, J. Zhu, J. Wang, X. H. Chen, and Y. Zhang, Nature **563**, 94 (2018).
[27] B. Huang, G. Clark, D. R. Klein, D. MacNeill, E. Navarro-Moratalla, K. L. Seyler, N. Wilson, M. A. McGuire, D. H. Cobden, D. Xiao, W. Yao, P. Jarillo-Herrero, and X. Xu, Nature Nanotechnol. **13**, 544 (2018).
[28] Z. Fei, W. Zhao, T. A. Palomaki, B. Sun, M. K. Miller, Z. Zhao, J. Yan, X. Xu, and D. H. Cobden, Nature **560**, 336 (2018).
[29] L. Liang, Q. Chen, J. Lu, W. Talsma, J. Shan, G. R. Blake, T. T. M. Palstra, and J. Ye, Sci. Adv. **4**, eaar2030 (2018).
[30] L. Liang, J. Shan, Q. H. Chen, J. M. Lu, G. R. Blake, T. T. M. Palstra, G. E. W. Bauer, B. J. van Wees, and J. T. Ye, Phys. Rev. B **98**, 134402 (2018).
[31] M. Guan, L. Wang, S. Zhao, Z. Zhou, G. Dong, W. Su, T. Min, J. Ma, Z. Hu, W. Ren, Z.-G. Ye, C.-W. Nan, and M. Liu, Adv. Mater. **30**, 1802902 (2018).
[32] M. Guan, L. Wang, S. Zhao, B. Peng, W. Su, Z. He, G. Dong, T. Min, J. Ma, Z. Hu, W. Ren, Z.-G. Ye, C.-W. Nan, Z. Zhou, and M. Liu, Adv. Funct. Mater. **29**, 1805592 (2019).
[33] S. D. Wang, Z. Z. Sun, N. Cue, H. Q. Xu, and X. R. Wang, Phys. Rev. B **65**, 125307 (2002).
[34] N. Bukar, S. S. Zhao, D. M. Charbonneau, J. N. Pelletier, and J.-F. Masson, Chem. Commun. **50**, 4947 (2014).
[35] C. Park, P. A. Fenter, N. C. Sturchio, and J. R. Regalbuto, Phys. Rev. Lett. **94**, 076104 (2005).
[36] P. García-Sánchez and A. Ramos, Phys. Rev. E **92**, 052313 (2015).
[37] G. Kresse and J. Hafner, Phys. Rev. B **47**, 558 (1993).
[38] G. Kresse and J. Furthmüller, Phys. Rev. B **54**, 11169 (1996).
[39] S. H. Vosko, L. Wilk, and M. Nusair, Can. J. Phys. **58**, 1200 (1980).
[40] P. E. Blöchl, Phys. Rev. B **50**, 17953 (1994).
[41] G. Kresse and D. Joubert, Phys. Rev. B **59**, 1758 (1999).
[42] H. J. Monkhorst and J. D. Pack, Phys. Rev. B **13**, 5188 (1976).
[43] E. H. Hall, Proc. Phys. Soc. Lond. **4**, 325 (1880).
[44] R. Karplus and J. M. Luttinger, Phys. Rev. **95**, 1154 (1954).
[45] T. Jungwirth, Q. Niu, and A. H. MacDonald, Phys. Rev. Lett. **88**, 207208 (2002).
[46] N. Nagaosa, J. Sinova, S. Onoda, A. H. MacDonald, and N. P. Ong, Rev. Mod. Phys. **82**, 1539 (2010).
[47] Y. Yao, L. Kleinman, A. H. MacDonald, J. Sinova, T. Jungwirth, D.-s. Wang, E. Wang, and Q. Niu, Phys. Rev. Lett. **92**, 037204 (2004).

[48] X. Wang, D. Vanderbilt, J. R. Yates, and I. Souza, Phys. Rev. B **76**, 195109 (2007).
[49] D. J. Thouless, M. Kohmoto, M. P. Nightingale, and M. den Nijs, Phys. Rev. Lett. **49**, 405 (1982).
[50] A. A. Mostofi, J. R. Yates, G. Pizzi, Y.-S. Lee, I. Souza, D. Vanderbilt, and N. Marzari, Comput. Phys. Commun. **185**, 2309 (2014).
[51] N. Marzari and D. Vanderbilt, Phys. Rev. B **56**, 12847 (1997).
[52] I. Souza, N. Marzari, and D. Vanderbilt, Phys. Rev. B **65**, 035109 (2001).
[53] N. Marzari, A. A. Mostofi, J. R. Yates, I. Souza, and D. Vanderbilt, Rev. Mod. Phys. **84**, 1419 (2012).
[54] Y. Yao and Z. Fang, Phys. Rev. Lett. **95**, 156601 (2005).
[55] G. Y. Guo, S. Murakami, T.-W. Chen, and N. Nagaosa, Phys. Rev. Lett. **100**, 096401 (2008).